

Subwavelength Focusing Using a Negative-Refractive-Index Transmission Line Lens

Anthony Grbic, *Student Member, IEEE*, and George V. Eleftheriades, *Senior Member, IEEE*

Abstract—We report simulations demonstrating subwavelength focusing of electromagnetic waves, from one homogeneous and isotropic dielectric to another, through a flat lens made of a realizable negative-refractive-index (NRI) metamaterial. The NRI metamaterial consists of a two-dimensional inductor, Capacitor (L,C) loaded transmission line (TL) network in a dual (high-pass) configuration. The microwave-circuit simulation results presented show that the voltage at the focal plane is identical to that at the source plane. The results confirm that in addition to focusing propagating waves, evanescent waves are also restored at the focal plane by the proposed loaded TL lens, thus enhancing the resolution of the image. In addition, the nature of the voltage distribution (vertical electric field) in this “perfect-focusing” setup is clarified.

Index Terms—Diffraction limit, evanescent waves, left-handed media, metamaterials, negative refractive index.

I. INTRODUCTION

CONVENTIONAL lenses focus electromagnetic waves by applying a phase correction to the propagating Fourier components, emanating from a source. The evanescent Fourier components which decay in amplitude away from the source, however, are lost and limit the image resolution of conventional lenses to approximately one wavelength. Recently, Pendry proposed a class of “perfect lenses” that achieve subwavelength focusing; these lenses correct the phase of propagating Fourier components but also restore the amplitudes of evanescent waves at the focal plane [1]. Pendry predicted that the flat slabs of negative-refractive-index (NRI) material (shown in Fig. 1), theoretically investigated by Veselago [2] in the 1960s, have the ability to restore evanescent waves and achieve subwavelength focusing. Pendry’s findings, which renewed interest in the peculiar properties of NRI media (“left-handed” media), were stimulated by the implementation of a composite structure exhibiting negative material parameters and, hence, a negative refractive index. The initial composite structure combined an array of metallic wires to attain negative permittivity and an array of split-ring resonators to achieve negative permeability [3]. It was used to demonstrate left-handed (backward-wave) propagation and experimentally verify negative refraction.

More recently, a periodic two-dimensional (2-D) inductor, Capacitor (L,C) loaded transmission line (TL) network [see

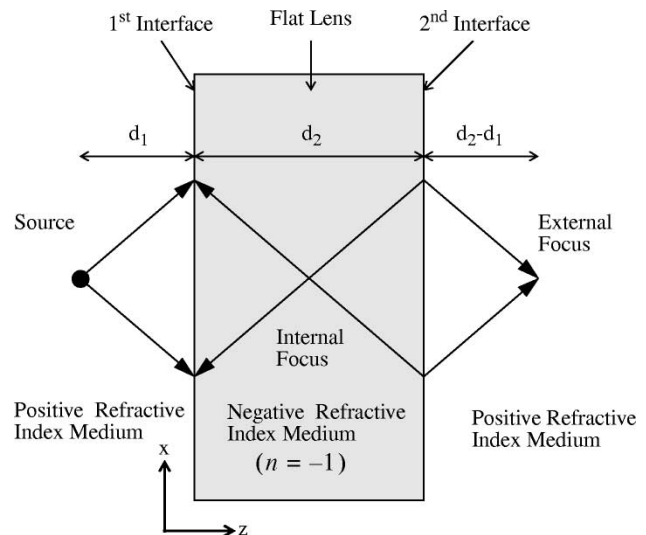


Fig. 1. Veselago’s negative refractive index flat lens system.

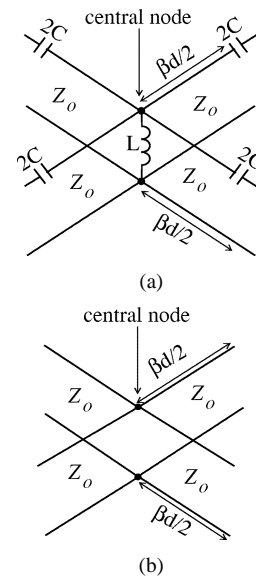


Fig. 2. TL unit cells. (a) NRI. (b) PRI.

Fig. 2(a)] was shown to exhibit properties associated with NRI media over a broad frequency bandwidth [4]. This network has been referred to as a dual TL structure due to its high-pass configuration, as opposed to the low-pass representation of a conventional TL [4], [5]. Backward wave radiation from the fundamental spatial harmonic [5], [6] and focusing were experimentally demonstrated at microwave frequencies using

Manuscript received May 27, 2003; revised July 3, 2003.

The authors are with the Edward S. Rogers Department of Electrical and Computer Engineering, University of Toronto, Toronto, ON M5S 3G4, Canada (e-mail: geleth@waves.utoronto.ca).

Digital Object Identifier 10.1109/LAWP.2003.819042

such dual TL structures [7], [8]. Simulation results have additionally been presented showing negative refraction and growing evanescent plane waves [4], [9], [10]. However, the subwavelength resolving properties that revived interest in NRI metamaterials have yet to be shown by any realizable structure. To date, studies have been predominantly theoretical assuming a continuous medium with uniform and isotropic negative permittivity and permeability [1], [11], [12]. In this letter, we present microwave-circuit simulation results of subwavelength focusing by a flat lens made of a dual TL (distributed) network—a realizable NRI metamaterial at microwave frequencies. The simulations are performed using Agilent’s Advanced-Design-System microwave circuit simulator and confirm that the three-region lens described in [10], which was shown to support growing evanescent waves, is indeed capable of achieving subwavelength focusing. It is important to note that the experimental lenses reported in [7], [8] utilized a single interface (two-region lenses) between a NRI medium and a positive refractive index (PRI) medium. This arrangement did not permit the proper growth of evanescent waves, necessary to clearly achieve subwavelength focusing. This leads to a dramatically different type of focusing when compared to [7], [8] as will be explained in the remainder of this letter.

Fig. 1 depicts the flat lens system envisioned by Veselago. Veselago showed that electromagnetic waves emanating from a source in a PRI medium can be focused using a rectangular slab of NRI metamaterial. The rays denote the negative refraction of the propagating Fourier components. This simple ray diagram suggests an internal focus within the slab itself and an external focus beyond the second slab interface in the PRI medium. The evanescent Fourier components, not shown in the figure, decay away from the source in the PRI media. Pendry discovered that these evanescent waves in fact grow inside the NRI medium such that they are restored to their original source amplitudes at the foci. The growing evanescent waves lead to large field amplitudes at the second interface. This “perfect focusing” involving the phase correction of propagating waves and the amplitude restoration of evanescent waves, only occurs when the NRI and PRI media have a relative refractive index of -1 with respect to each other and are impedance matched.

II. NEGATIVE-REFRACTIVE-INDEX TRANSMISSION-LINE LENS

The PRI medium considered in this letter is a TL mesh composed of the unit cells shown in Fig. 2(b). The NRI medium, on the other hand, is made up of the dual TL unit cells depicted in Fig. 2(a). Both the TL mesh and dual TL structure operate in regions of homogeneous and isotropic propagation (long wavelength regime) and can be considered as effective media [4], [9]. It is important to clarify that the unit cells for both PRI and NRI media depicted in Fig. 2 are of finite size d which is determined by the interconnecting TLs. Therefore, the resulting media are not just mere networks of lumped elements: they do have a finite length and thus wave propagation in them and a corresponding wavelength can be unambiguously defined. At the frequency of operation, the dual TL structure exhibits backward wave propagation, characteristic of a NRI medium, while the TL mesh exhibits forward-wave propagation, characteristic

of a PRI medium. For simplicity, the same TL sections are used in both the NRI [Fig. 1(a)] and PRI [Fig. 1(b)] media. Therefore, the unit cells differ only in terms of the loading L, C components in the dual TL structure. To achieve a relative refractive index of $n = -1$, the effective wavenumbers of the TL mesh and dual TL structure are set equal in magnitude but opposite in sign. The dispersion relations for the dual TL structure and the TL mesh are given by (1) and (2), respectively [9]

$$\begin{aligned} \sin^2\left(\frac{k_{xn}d}{2}\right) + \sin^2\left(\frac{k_{zn}d}{2}\right) &= \frac{1}{2} \left[2 \sin\left(\frac{\beta d}{2}\right) - \frac{1}{Z_o \omega C} \cos\left(\frac{\beta d}{2}\right) \right] \\ &\quad \times \left[2 \sin\left(\frac{\beta d}{2}\right) - \frac{Z_o}{2\omega L} \cos\left(\frac{\beta d}{2}\right) \right] \end{aligned} \quad (1)$$

$$\begin{aligned} \sin^2\left(\frac{k_{xp}d}{2}\right) + \sin^2\left(\frac{k_{zp}d}{2}\right) &= 2 \sin^2\left(\frac{\beta d}{2}\right) \end{aligned} \quad (2)$$

where k_{xn} and k_{zn} are the transverse and longitudinal wavenumbers in the dual TL structure respectively, while k_{xp} and k_{zp} are the transverse and longitudinal wavenumbers in the TL mesh respectively. Furthermore, ω is the radial frequency, d is the unit cell dimension, β is the propagation constant of the interconnecting TL sections and Z_o is their characteristic impedance, L is the shunt loading inductance and C is the series loading capacitance in the dual TL structure. In addition, the Bloch impedances for the TL mesh (PRI medium) and dual TL structure (NRI medium) are set equal to each other. This provides an impedance match between the two media eliminating reflections at the interfaces. The Bloch impedances in the x and z directions for the dual TL structure are given by the following [9]:

$$Z_{xn} = \frac{Z_o \tan\left(\frac{\beta d}{2}\right) - \frac{1}{2\omega C}}{\tan\left(\frac{k_{xn}d}{2}\right)}, \quad Z_{zn} = \frac{Z_o \tan\left(\frac{\beta d}{2}\right) - \frac{1}{2\omega C}}{\tan\left(\frac{k_{zn}d}{2}\right)}. \quad (3)$$

Similarly, the Bloch impedances in the x and z directions for the TL mesh are [9]

$$Z_{xp} = Z_o \frac{\tan\left(\frac{\beta d}{2}\right)}{\tan\left(\frac{k_{xp}d}{2}\right)}, \quad Z_{zp} = Z_o \frac{\tan\left(\frac{\beta d}{2}\right)}{\tan\left(\frac{k_{zp}d}{2}\right)}. \quad (4)$$

The electrical parameters of a TL mesh and dual TL structure that are impedance matched and have a relative refractive index of $n = -1$ with respect to each other at 1 GHz, are shown in Table I.

III. SUBWAVELENGTH FOCUSING

Microwave circuit simulations of a finite size structure consisting of a dual TL (NRI) lens sandwiched between two TL mesh (PRI) media (as shown in Fig. 1) were performed to verify subwavelength focusing. In the simulations, the TL meshes extended 19 cells (rows) in the x direction and 12 cells (columns) in the z direction. The dual TL lens extended 19 cells (rows) in

TABLE I
ELECTRICAL PARAMETERS FOR THE TL MESH AND DUAL TL STRUCTURE AT 1 GHz

kd	Z_o	βd	L	C
0.3491 rad	71.2573 Ω	0.2462 rad	11.4500 nH	4.513 pF

the x direction and five cells (columns) in the z direction. A 1 V (0 dB) generator oscillating at 1 GHz was connected to the central node of cell [column, row] = [10, 10] to act as a source of cylindrical waves in the PRI medium. Consequently, the TL mesh acts as a parallel-plate radial guide in its TL (TM_{00}) mode of operation. The voltages and currents take on a radial variation of the form $H_0^{(2)}(kr)$ and $H_1^{(2)}(kr)$, respectively (Hankel functions of the second kind, assuming an $e^{j\omega t}$ time harmonic variation), where $r = \sqrt{x^2 + z^2}$ is the distance from an observation point (z, x) relative to the source. The effective propagation constant k (see Table I) is given by the following:

$$k^2 = k_{xp}^2 + k_{zp}^2 = k_{xn}^2 + k_{zn}^2. \quad (5)$$

The impedance at the terminals of a unit cell located at (z, x) from the source can, therefore, be approximated by the following radial TL impedance formulas:

$$Z_{rx}(r) = \frac{-jZH_0^{(2)}(kr)}{H_1^{(2)}(kr)} \frac{x}{r} \quad (6)$$

$$Z_{rz}(r) = \frac{-jZH_0^{(2)}(kr)}{H_1^{(2)}(kr)} \frac{z}{r} \quad (7)$$

where Z_{rx} is the x directed and Z_{rz} the z directed radial TL impedance. The edges of the first TL mesh parallel to the z axis and those parallel to the x axis were terminated in lumped impedances computed using (6) and (7), respectively. The dual TL lens (NRI medium) and second TL mesh (PRI medium) were terminated in radial TL impedances computed with respect to the internal and external foci, respectively.

Fig. 3 depicts the voltage magnitudes in decibels at the central nodes of all the unit cells in the PRI and NRI media. An internal focus [column, row] = [15, 10] in the dual TL structure (NRI medium) and an external focus [column, row] = [20, 10] in the TL mesh (PRI medium) are designated based on the ray picture of Fig. 1. High voltage amplitudes are evident at the second interface due to the growing evanescent waves in the dual TL structure: although Fig. 3 shows the total field distribution consisting of both propagating and evanescent wave contributions, the growth of evanescent waves alone was demonstrated in a similar three-region lens setup in [10].

To further clarify the nature of focusing in this three-region lens setup, the phase distribution of the nodal voltages is shown in Fig. 4. This is a very revealing plot. First, one should observe that the exterior wavefronts (i.e., the ones further away from the central row 10) clearly form three distinct cylindrical waves. By inspection, the phase centers of these cylindrical wavefronts are located at the source, the internal focus and the external focus, as were designated in Fig. 3. Therefore, the internal and external foci can be uniquely identified from this phase plot. Furthermore, between the internal and external foci, an elongated region of constant-phase variation is formed along central row 10.

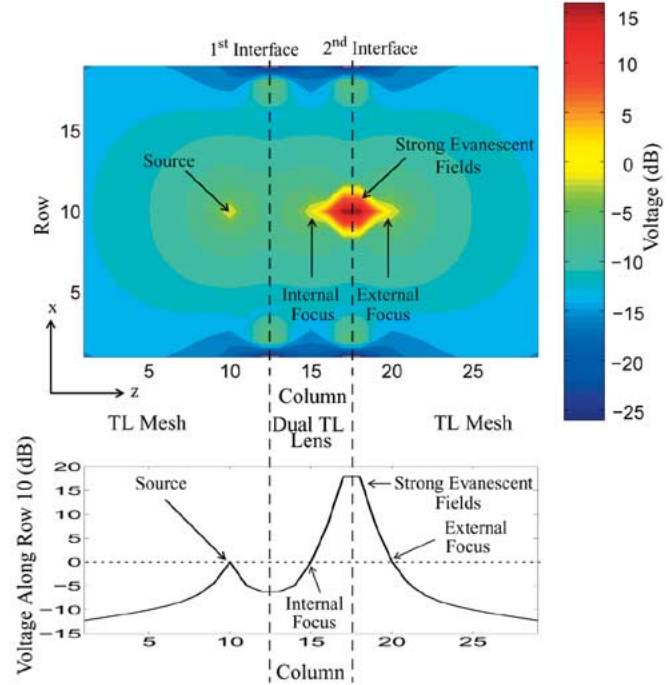


Fig. 3. Simulated focusing results at 1 GHz (voltage amplitudes).

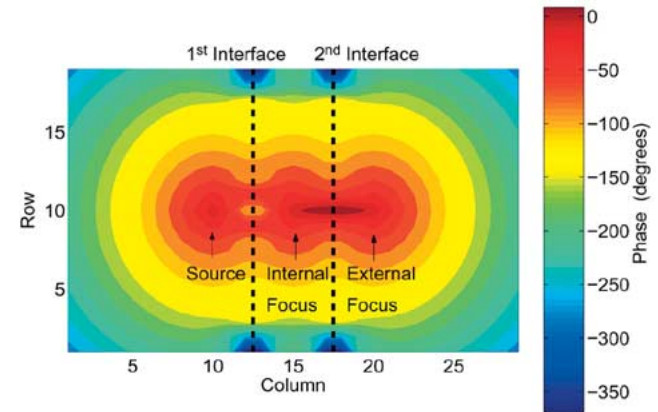


Fig. 4. Simulated focusing results at 1 GHz (voltage phase).

This is consistent with the notion that this region is dominated by evanescent waves.

Having identified the external focus from Fig. 4, the voltage amplitudes at the external focal plane are plotted against the voltage amplitudes at the source plane in Fig. 5. As shown, the two voltage distributions are identical signifying the recreation of the source voltage distribution along the focal plane at 1 GHz. This situation is indicative of subwavelength focusing. In other words, the voltage distribution at the source plane is exactly reconstructed at the image plane, including any subwavelength features. For example in Fig. 5, the sharp peak of the source

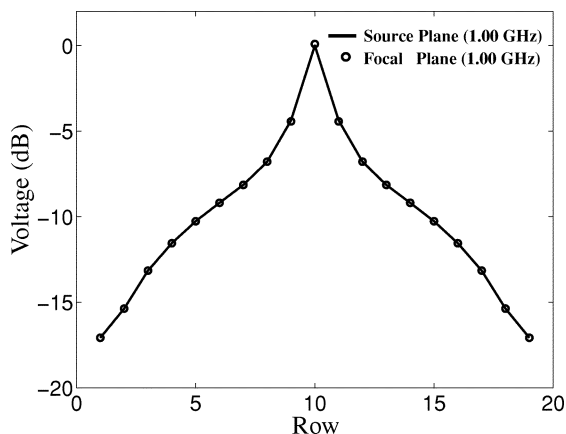


Fig. 5. Voltage amplitudes at the source plane (column 10) and external focal plane (column 20).

about row 10 is exactly reproduced at the image plane; This should be placed in the context of the fact that these details are on the order of a unit cell which is only about $\lambda/20$ (see Table I). Specifically, the 3-dB beamwidth of the image is 1.37 cells or equivalently about $1/13$ effective wavelengths (27.4°).

Note that this kind of focusing in a three-region TL NRI lens is dramatically different than the focusing previously observed in the two-region TL lenses of [7], [8] in that the former is dominated by evanescent waves. This leads to subwavelength resolution at the external focal point, which incidentally does not coincide with the point of maximum amplitude. Furthermore, it should be pointed out that an intriguing anisotropic TL structure that experimentally achieved subwavelength focusing is described in [13]. In that structure, no evanescent waves are involved, however both the source and its image should be embedded in (complementary) anisotropic metamaterials thus precluding imaging in free space.

IV. CONCLUSION

In this letter, we have presented simulations demonstrating subwavelength focusing of electromagnetic waves, from one homogeneous and isotropic dielectric to another through a realizable NRI lens consisting of a periodic 2-D L,C loaded TL network. These microwave circuit simulation results, clearly

demonstrate that the voltage along the external focal plane is identical to that of the source. These results indicate that in addition to focusing propagating waves, the evanescent fields are also restored by the dual TL lens. Strong voltage amplitudes at the lens' second interface confirm that evanescent waves grow inside the lens and as a result contribute to the image resolution. These findings clarify the nature of Pendry's "perfect" imaging when the lens is lossless, impedance matched and exhibits a relative refractive index of $n = -1$.

REFERENCES

- [1] J. B. Pendry, "Negative refraction makes a perfect lens," *Phys. Rev. Lett.*, vol. 85, pp. 3966–3969, Oct. 2000.
- [2] V. G. Veselago, "The electrodynamics of substances with simultaneously negative values of ϵ and μ ," *Sov. Phys. Usp.*, vol. 10, pp. 509–514, Jan.–Feb. 1968.
- [3] R. A. Shelby, D. R. Smith, and S. Schultz, "Experimental verification of a negative index of refraction," *Sci.*, vol. 292, pp. 77–79, Apr. 2001.
- [4] A. K. Iyer and G. V. Eleftheriades, "Negative refractive index metamaterials supporting 2-D wave propagation," in *IEEE MTT-S Int. Microwave Symp. Dig.*, vol. 2, Seattle, WA, June 2002, pp. 1067–1070.
- [5] A. Grbic and G. V. Eleftheriades, "A backward-wave antenna based on negative refractive index L-C networks," in *IEEE Int. Symp. Antennas Propagat.*, vol. 4, San Antonio, TX, June 2002, pp. 340–343.
- [6] —, "Experimental verification of backward-wave radiation from a negative refractive index metamaterial," *J. Appl. Phys.*, vol. 92, pp. 5930–5935, Nov. 2002.
- [7] G. V. Eleftheriades, A. K. Iyer, and P. C. Kremer, "Planar negative refractive index media using periodically L-C loaded transmission lines," *IEEE Trans. Microwave Theory Tech.*, vol. 50, pp. 2702–2712, Dec. 2002.
- [8] A. K. Iyer, P. C. Kremer, and G. V. Eleftheriades, "Experimental and theoretical verification of focusing in a large, periodically loaded transmission line negative refractive index metamaterial," *Optics Express*, vol. 11, pp. 696–708, Apr. 2003.
- [9] A. Grbic and G. V. Eleftheriades, "Periodic analysis of a 2-D negative refractive index transmission line structure," *IEEE Trans. Antennas Propagation (Special Issue: Metamaterials)*, vol. 51, Oct. 2003, to be published.
- [10] —, "Growing evanescent waves in negative-refractive-index transmission-line media," *Appl. Phys. Lett.*, vol. 82, pp. 1815–1817, Mar. 2003.
- [11] N. Fang and X. Zhang, "Imaging properties of a metamaterial superlens," *Appl. Phys. Lett.*, vol. 82, pp. 161–163, Jan. 2003.
- [12] R. W. Ziolkowski and E. Heyman, "Wave propagation in media having negative permittivity and permeability," *Phys. Rev. E*, pp. 056 625/1–056 625/15, Nov. 2001.
- [13] K. G. Balmain, A. E. Luttgen, and P. C. Kremer, "Resonance cone formation, reflection, refraction and focusing in a planar, anisotropic metamaterial," *IEEE Antennas Wireless Propagat. Lett.*, vol. 1, pp. 146–149, Dec. 2002.